https://doi.org/10.1016/j.nanoen.2020.105724

Environment-resisted Flexible High Performance Triboelectric Nanogenerators based on Ultrafast Self-healing Non-drying Conductive Organohydrogel

Long-Biao Huang[a, 1]*, Xingyi Dai[b,1], Zhenhua Sun[a], Man-Chung Wong[c], Sin-Yi Pang[c], Jiancheng Han[a], Qiuqun Zheng[a], Cheng-Han Zhao[a], Jie Kong[b, *] and Jianhua Hao[c, *]

[a] Dr L.-B. Huang, Dr Z. Sun, J. Han, Q. Zheng, C.-H. Zhao
Key Laboratory of Optoelectronic Devices and Systems of Ministry of Education and Guangdong Province, College of Physics and Optoelectronic Engineering, Shenzhen University, Shenzhen, 518060, P. R. China
* Corresponding Author, E-mail: huanglb@szu.edu.cn

[b] X. Dai, Prof J. Kong
MOE Key Laboratory of Materials Physics and Chemistry in Extraordinary Conditions, Shaanxi Key Laboratory of Macromolecular Science and Technology, School of Chemistry and Chemical Engineering, Northwestern Polytechnical University, Xi'an, 710072, P. R. China
* Corresponding Author, E-mail: kongjie@nwpu.edu.cn

[c] Sin-Yi Pang, Dr M.-C. Wong, Prof J.H. Hao
Department of Applied Physics, The Hong Kong Polytechnic University, Hong Kong, China
* Corresponding Author, E-mail: jh.hao@polyu.edu.hk

[1] The authors contributed equally to this work.

Highlights

- An environment-resisted, icephobic, and ultrafast self-healing triboelectric nanogenerator (TENG) with excellent electrical outputs has been developed.
- Based on the anti-freezing and non-drying organohydrogel, the TENG can survive at a broad temperature range from -30 ^{o}C to 80 ^{o}C.
- The ultrafast self-healing function enables the device output performance timely recover without delay.

Abstract

Triboelectric nanogenerator (TENG), a promising energy harvesting technique, has attracted intense research interests in recent years for its applicability in portable and wearable electronics. Self-powered sensors with high sensitivity based on TENG have been widely reported. However, for practical applications, the survivability of TENG in harsh working environments is a vital issue which must be addressed. Herein, we report a hydrophobic, icephobic, and ultrafast self-healing TENG with outstanding non-drying and non-freezing properties for energy harvesting and self-powered sensor. Due to the excellent environment resist and conductive capability of organohydrogel, the TENG shows much better electrical output stability in a wide temperature range than conventional hydrogel-based TENG which suffers from being frozen at low temperature and dried at high temperature. Moreover, the ultrafast self-healing function enables the electrical output performance of the TENG rapidly restore without delay. The TENG in this work demonstrates an open-circuit voltage of 157 V, a short-circuit current of 16 μA, and a short-circuit charge of 29 nC. The maximum output power density reaches up to 710 mW m^{-2}. This research might pave a new road for novel applications of TENG in harsh environments with reliable output performance and self-healing capability for practical applications.

Keywords: Triboelectric nanogenerators, Environment-resisted, Self-healing, Non-drying, Organohydrogel.

1. Introduction

Due to the finiteness of traditional fossil fuel as well as the environmental issues, harvesting technologies for different green energy have been developed and attained great achievements [1-4]. Among those techniques, nanogenerator as a novel mechanical energy harvesting technology has attracted amounts of attentions from academics and industrial pools due to its advantages of low cost, high performance, easy fabrication, and so on [5, 6].

As one type of nanogenerators, triboelectric nanogenerators have shown tremendous advantages in mechanical energy harvesting and self-powered sensors [5, 7]. With lots of efforts from academic community devoted, the performance and stability of the TENG has been significantly improved, enabling its application in a variety of areas, like self-powered sensors [8-13]. On the other hand, for the practical application, the good survivability of a TENG in multiple environments such as different temperature, high dusts, mechanical impact, and moisture is indispensable [14, 15]. For example, high temperature could deteriorate the mechanical properties of device materials. Low temperature could not only worsen the mechanical properties of device materials, but also lead to the moisture absorption from air and form water or ice layer on the surface of device. At the same time, TENG could suffer from different mechanical impact which lead to serious damage of device materials in real operation. Meanwhile, high dusts could contaminate the contact surface of TENG and decrease the output performance of device.

To address above issues, various methodologies regarding novel materials and device structure have been investigated [9, 15-20]. To reduce thermal influence, Wang et.al demonstrated an environmentally stable TENG by introducing an ionic conductor electrode, which could maintain stable up to 335 ^{o}C [21]. You et.al. applied iongel in TENG, realizing a stable performance with temperature up to 100 ^{o}C, as well as great stretchability and durability [22]. However, there is lack of report on how to avoid ice accretion on the surface of devices at low temperature, which could decrease the output performance and lifetime of TENGs. To avoid the contamination of dusts, hydrophobic property was introduced on the surface of device to stabilize the output performance of TENG from dusts [23]. Xu et.al. introduced a PVA hydrogel-based TENG with high performance and excellent recyclable properties to enhance the survivability from mechanical impact. The recycled device in the report can retain 92% of the output performance of the original one [9]. However, merely reports have performed the systematically investigation and given the environment-resistant capability to TENG.

Among diverse materials of TENG, the gel with excellent mechanical properties, biocompatibility, biodegradability, and super self-healing capability might be a good candidate to endow TENG with high environment resist [9, 21, 24-26]. Hydrogel with excellent properties has been applied in TENG [17, 22]. However, the drying and freezing processes suffered on the hydrogel would lead to the evaporation and

crystallization of water molecular, which could seriously constrain the working temperature range of TENG, and shorten the lifetime of device.

Herein, we demonstrate a hydrophobic, icephobic, and ultrafast self-healing TENG with thermal-resist, non-drying, and non-freezing properties. The novel TENG could survive at a wide temperature range from -30 ºC to 80 ºC. The hydrophobic and icephobic properties suppress the accretion of water and ice layer on the surface of device. The presented TENG shows good electrical output stability across a broad temperature range than conventional hydrogel-based TENG. The output performance of novel TENG could achieve at about 157 V, 16 μA and 29 nC of the open-circuit voltage, short-circuit current and short-circuit charge, respectively. The maximum value of output power density could achieve at 710 mW m^{-2}. The self-healing property of device provides TENG with excellent recovery of electric output, which could be restored to the initial state within 1 s in a broad temperature range. The fast healing rate enables the output performance of the broken device without delay during the repair process. Considering all of these advantages, this research shows a promising possibility of TENG in harsh environments with reliable output performance and self-healing capability for practical applications. This technology provides not only physical protection from the surroundings, but also thermal and mechanical isolation to enhance device performance.

2. Experimental Section

2.1. Materials

Acrylamide (AAM), potassium persulfate (KPS), glycerol, N,N,N',N'-tetramethylethylenediamine (TEMED), and other chemicals were purchased from Sigma-Aldrich. Bis(3-aminopropyl) terminated poly(dimethylsiloxane) (NH_2-PDMS-NH_2, M_n = 5000–7000) was purchased from Gelest. Synthetic hectorite clay (Laponite XLS) was provided by BYK Ltd. All chemicals were used as received without further purification. Besides, 1,1,1-tris[(4-formylphenoxy)methyl]ethane and 2(6-isocyanatohexylaminocarbonylamino)-6-methyl-4[1H]pyrimidinone were synthesized as previously reported [27, 28].

2.2. Synthesis of Organohydrogel

The cross-linked hydrogel was synthesized as following: Laponite XLS (1 g) was dispersed in DI water (6 ml) under ultrasonication for 1 hr and then magnetically stirred for 2 hr. Subsequently, AAM (1 g) was added and the solution was stirred for another 0.5 hr. After that, 1 mL of KPS aqueous solution (0.015 g mL^{-1}) and 20 μL of TEMED were added into the solution successively, followed by stirring for an additional 0.5 hr. Then, the whole solution was poured into PTFE petri dish. After curing for about 24 hr at room temperature, the as-prepared cross-linked hydrogel named PAAM-Clay hydrogel was peeled off from PTFE petri dish and cut into a suitable dimension for subsequent use. To obtain an anti-freezing, non-drying, and conductive organohydrogel, a solvent displacement was performed upon the

PMMA-Clay hydrogel according to the literature with modification [29]. Specifically, PAAM-Clay hydrogel was placed in beak filled with an amount of glycerol for 12 hr. The obtained PAAM-Clay organohydrogel was washed using glycerol. Then, the specimens were cleared by a filter paper.

2.3. Synthesis of IU-PDMS

IU-PDMS was synthesized using the method reported before [28]. 2(6-Isocyanatohexylaminocarbonylamino)-6-methyl-4[1H]pyrimidinone (0.06 g, 0.2 mmol) was added to the solution of bis(3-aminopropyl) terminated poly(dimethylsiloxane) (3 g, 0.6 mmol) in 15 mL of $CHCl_3$. The mixture was heated at 60 ºC under reflux for 6 h. When the solution was cooled to room temperature, 1,1,1-tris[(4-formylphenoxy)methyl]ethane (0.152g, 0.333 mmol) was added. Then the solution was stirred for overnight. The solution was cast on a Teflon mold and dried for 24 h at room temperature and 60 °C successively in a vacuum oven.

2.4. Fabrication of Device

The TENGs were fabricated with the following steps. Firstly, the organohydrogel and IU-PDMS were cut into a suitable dimension. Then a sandwich structure was constructed using two IU-PDMS films (thickness of 0.5 mm) and single organohydrogel layer (thickness of 1 mm). IU-PDMS functioned as tribomaterials, and organohydrogel was employed as the electrode and device supporting material. For comparison, a TENG in the same structure with hydrogel and IU-PDMS film

were also fabricated. The device based on organohydrogel and hydrogel were named organohydrogel-TENG (OG-TENG) and hydrogel-TENG (HG-TENG), respectively.

2.5. Characterization

The infrared thermal images were recorded by Fluke Ti25 infrared camera. The mechanical tensile tests were conducted on a universal tester (Instron 3342) with a strain rate of 20 mm min^{-1} according to ISO37-4. The contact angles were measured using a contact angle analyzer (DSA100S, KRUSS). X-ray photoelectron spectroscopy (XPS) measurement was conducted on a K-Alpha spectrometer (Kratos Axis Ultra DLD) and the core level spectra were measured using a monochromatic Al Kα X-ray source ($h\nu$ = 1486.6 eV) with the energy resolution of 0.45 eV (Ag 3d 5/2). Scanning electron microscopy (SEM) and elemental mapping images were performed on a field emission scanning electron microscope (FEI Verios G4). Atomic force microscope (AFM, Bruker Dimension Icon) was utilized to characterize the surface morphology of polymer. Resistance measurements were performed on a source meter (Keithley 2450). The open-circuit voltage (V_{oc}), short-circuit current (I_{sc}) and short-circuit charge (Q_{sc}) of TENGs were measured by LeCroy Wave Runner Oscilloscope (44MXI) with probe resistance value of 10 MΩ, SR570 low noise current amplifier (Stanford Research System) and 6514 system electrometer (Keithley). Differential scanning calorimetry (DSC) was performed using a Mettler Toledo DSC 1 instrument to determine glass transition temperatures (T_g) from -80 ^oC to 120 ^oC with a heating rate of 10 $^oCmin^{-1}$. The ice adhesion strength was measured

as the reference [30]. A cuvette (10 mm × 10 mm × 45 mm) with 2 mL deionized water was placed onto the sample, followed by transferring into a refrigerator at -18 ^{o}C for 12 h to ensure the water completely frozen on the sample surface. Then the sample was transferred to a cold plate to maintain the temperature of sample surface below -10 ℃. The force transducer (SUNDOO, SH-50) was able to move at a constant speed of 2 mm s^{-1} to propel the cuvette. The peak value of force was recorded, which was divided by contact area to calculate the ice adhesion strength [31].

3. Results and Discussion

3.1. Synthesis of Organohydrogel and IU-PDMS

The synthesis processes of organohydrogel and triboelectric layer were designed and experimentally carried out as the following processes shown in Fig. 1. Firstly, the cross-linked hydrogel based on hydrogen bond was synthesized by mixture of AAM and clays. After adding KPS and TEMED, the curing processes were initiated as shown in Fig. 1a. And then, the specimen was immersed in the glycerol for solvent displacement [29], as shown in Fig. 1b. After removing the water in hydrogel, the glycerol could fully penetrate the cross-linked polymer matrix and form organohydrogel. The self-healing triboelectric materials were designed and synthesized as shown in Fig. 1c. A certain amount of 2(6-isocyanatohexylaminocarbonylamino)-6-methyl-4[1H]pyrimidinone was grafted to the end of bis(3-aminopropyl) terminated poly(dimethylsiloxane), which was then reacted with 1,1,1-tris[(4-formylphenoxy)methyl]ethane. Cross-linked by imine bond

and quadruple hydrogen bonding (UPy), the flexible and healable poly(dimethylsiloxane) (IU-PDMS) elastomer was obtained, which was consistent with our previous results [28].

3.2. Anti-freezing and Non-drying Properties of Organohydrogel

The material properties were systematically studied after synthesis. The anti-freezing and thermal-resistant property of the as-prepared organohydrogel and hydrogel were measured. At room temperature (25 ^{o}C), the hydrogel and organohydrogel show similar properties with good bendability without any breaking (Fig. 2a and 2d). When the hydrogel and organohydrogel specimens were put into -30 ^{o}C for 2 hr, the hydrogel can be easily broken into two fragments due to the crystallization of water, as shown in Fig. 2e. On the other hand, the organohydrogel still keeps good bendability without any change in Fig. 2b, as the glycerol has replaced water molecular during solvent displacement. When the two kinds of specimens were stored in oven at 80 ^{o}C for 30 mins, the hydrogel can be easily broken into many fragments in Fig. 2f. In contrast, the organohydrogel still holds great bendability, as shown in Fig. 2c. Noteworthily, even undergoing multiple heating and cooling process, the organohydrogel still maintained its original performance with good flexibility, and exhibited excellent stability.

3.3. Self-healing Properties of Organohydrogel and IU-PDMS

During the operation of TENG in practical applications, the device has to undergo

different mechanical impacts in a range of temperatures. Therefore, the TENG with self-healing properties promises wide applications. In this study, IU-PDMS functions as tribomaterial, and the organohydrogel functions as the electrode and supporting material of a device. To investigate the self-healing properties of organohydrogel and IU-PDMS, the qualitative characterization and quantitative uniaxial tensile tests were performed. For each material, two pads marked with different colours were separately cut into two pieces. Parts from different pads were linked forming a full contact at room temperature. As shown in Fig. 3a and 3b, the two parts are tightly jointed through the self-healing reaction in their cross-sections, indicating their excellent self-healing properties. Fig. 3a presents that the organohydrogel can achieve self-healing and form one part that cannot be separated by bending and stretching. Similarly, the self-healed IU-PDMS can be bent and twisted, as shown in Fig. 3b. The tensile strain curves of organohydrogel and IU-PDMS were further investigated to ascertain their mechanical properties after self-healing. As shown in Fig. 3c, the original organohydrogel shows a strength of 0.25 MPa and a breaking strain of 3360%. After healing for 1 min, the specimen can reach a strength of 0.23 MPa and a breaking strain of 3310%. The IU-PDMS has strength of 1.22 MPa and breaking strain of 228%. The self-healed specimen of IU-PDMS in 24 hr has strength of 1.20 MPa and breaking strain of 221% (Fig. 3d). Our materials exhibited excellent mechanical self-healing characteristics, which could be ascribed to the reversible covalent and noncovalent interactions in the cross-linking networks. For PAAM-Clay organohydrogel, there were hydrogen bonds between PAAM chains and clay. For

IU-PDMS, imine bonds and UPy units could synergistically promote self-healing process. The broken imine bonds could be reformed, and the hydrogen bonds and UPy dimers had the characteristic of dynamic association-dissociation, resulting in the self-healing of two polymers. Meanwhile, organohydrogel and IU-PDMS were soft at room temperature with low glass-transition temperature (T_g, < -50 ^oC), which was allowing for the mobility of molecular chain to facilitate bonding the fractured interfaces [32].

To further investigate the electrical self-healability of the organohydrogel, the two parts with different colors were connected into a circuit in series with an LED bulb and DC power source, as shown in Fig. 3e. When the two separated organohydrogel parts were brought together and a voltage of 5 V was applied, the green LED bulb was lighted up, indicating the circuit was restored through the self-healing process of the organohydrogel. Next, the self-healing performance of organohydrogel at different temperature was investigated. Fig. 3f presents the change of resistance during the process of cut and contact at different temperature. The resistance was about 87 kΩ, 54 kΩ, and 33 kΩ at -30 ^oC, 25 ^oC, and 80 ^oC, respectively. After the organohydrogel being completely cut into half, the resistance became infinite. Once the two parts were reattached together, the resistance declined rapidly and recovered to their initial states within 1 s at three different temperature. The weak noncovalent hydrogen bonds could be easily disassociated and associated. Moreover, the T_g of the organohydrogel was below -80 ^oC and it contained liquid glycerol, signifying enough mobility of polymer

segment, which promoted the association of hydrogen bonds and achieved rapid self-healing even at -30 ^{o}C. By rising temperature, molecular activity increased. Therefore, the healing process was easier at higher temperature. The results demonstrate that the organohydrogel has good conductivity and ultrafast electrical self-healability in a broad temperature range, which is in favour of being applied in electronic devices.

3.4. Icephobic Properties of IU-PDMS

As the TENG is supposed to operate in a real environment, the external pollutants such as dusts, water, and ice could influence the output performance of the device. Especially, depending on temperature and humidity, there could be a water or ice layer formed on the surface of a TENG. To minimize this influence, a hydrophobic and icephobic surface of the TENG is of great need [33]. Therefore, the hydrophobic and icephobic properties of IU-PDMS were characterized. As illustrated in Fig. 4a, the contact angle of the IU-PDMS is about 113^{o}, indicating the surface is hydrophobic. The original IU-PDMS displays a low ice adhesion strength of 9 kPa. After sliding by a doctor blade, the ice adhesion strength increases to 68 kPa, due to the appearance of scratches. The water could penetrate into the crack, resulting in mechanical interlocking at the interface after freezing and enhancing the ice adhesion strength. After the broken sample being self-healed at room temperature for 24 hr, the ice adhesion strength recovers to 12 kPa. Ice adhesion strength is an important parameter to evaluate icephobic properties. When the ice adhesion strength of the surface is

below 100 kPa, it can be considered icephobic [34]. Under supercooled conditions, freezing is an inevitable phenomenon. The low ice adhesion strength means that even if ice layer eventually forms on the surface, the ice can be easily removed. The hydrophobic and icephobic properties could be attributed to the chemical element of Si and smooth surface [33]. Fig. 4b and 4c illustrate rich Si elements on the surface of IU-PDMS. XPS spectra present the significant 2s and 2p peaks of Si. The element mapping images confirm the appearance of Si and other chemical elements. Ice adhesion strength is proportional to surface energy. Therefore, the chemical element of Si with low surface energy is in favour of improving the icephobicity. SEM image in Fig. 4c shows the smooth surface of IU-PDMS, which is further confirmed by the low roughness of AFM image in Fig. 4d. The smooth surface might avoid mechanical interlocking between the substrate and ice. Sometimes the ice adhesion strength of flat hydrophobic surface is much lower than that of superhydrophobic surface with micro-nanoscale texture [35]. Moreover, the IU-PDMS was soft, while ice was stiff, leading to air voids formed at the interface. The voids serving as stress concentrators could initiate crack growing and facilitate the detachment of ice from the surface under shearing forces. Therefore, due to the chemical structure, flexibility and smooth surface, IU-PDMS presented excellent hydrophobic and icephobic properties. Meanwhile, the self-healing capability of IU-PDMS could prevent the interlocking at the interface between mechanically damaged material and ice, thus guaranteeing good icephobicity, which was beneficial for the lifetime of TENG based on IU-PDMS in harsh environments.

3.5. Working Mechanisms and Output Performances of Devices

After the systematically investigation on the intrinsic properties of the IU-PDMS and organohydrogel, the single-electrode mode organohydrogel-based TENG (OG-TENG) was designed and fabricated, as shown in Fig. 5a and Fig. S1 provided in Supplementary Information. The operation principle of TENG device is presented in Fig. 5b. Due to the differences in electron affinity between various materials, the tribo-electrification could occur at the interface between the skin and IU-PDMS. The same amount of positive and negative charges could be separately generated at the surface of skin and IU-PDMS, as shown in Fig. 5a-i. When the skin is separated from the IU-PDMS, the tribo-charges at the surface of IU-PDMS could induce the migration of ion in the organohydrogel to keep the electric neutrality, as shown in Fig. 5a-ii. Meanwhile, the same amount of opposite charges at the interface between organohydrogel and metal electrode could be generated due to polarization of electrical double layer at the same interface in which the electrical double layer could form. To satisfy the electrical double layer, electrons will flow to the ground through the external circuits (Fig. 5a-iii). When the skin is approaching to the device as shown in Fig. 5a-iv, electron flux will return from the ground to the interface between organohydrogel and electrode. By repeating the contact-separation process, an alternating current (AC) can be generated, converting the mechanical energy into electricity or electrical signals.

The output performance of the single-electrode OG-TENG was measured with an active area of 4 × 4 cm^2 between the skin and device. As shown in Fig. 5b-5d, the open-circuit voltage (V_{oc}), short-circuit current (I_{sc}), and short-circuit charge (Q_{sc}) are about 157 V, 16 μA, and 29 nC, respectively. The load resistance dependent V_{oc} and I_{sc} of the OG-TENG are presented in Fig. 5e. With the increase of loading resistance, the V_{oc} increases, while I_{sc} decreases. The maximum output power density is attained at 710 mW m^{-2} with the load resistance of 20 MΩ which is equal to the inherent impedance of TENG (Fig. 5f). Without an external storage device, the device could easily light 30 green LEDs up, as shown in Fig. 5g. The relative results in Fig. 5 demonstrate the capability of the device to convert mechanical energy into electricity.

3.6 Environment-resisted and Self-healing Devices

In the previous studies, the TENGs with solvent-free ion-conducting elastomer electrode and iongel have been demonstrated to excellent thermally stability with high temperature up to 335 ^oC and 100 ^oC, respectively [21, 22]. At the same time, self-healing property and icephobicity at low temperatures are also important for TENGs to be utilized in harsh environments. As discussed above, the water was removed through solvent displacement, leading to the anti-freezing and non-drying properties of the organohydrogel electrode. Owing to the chemical element of Si with low surface energy, smooth surface, and flexibility, the IU-PDMS elastomer as tribomaterial was hydrophobic and icephobic. Moreover, both the organohydrogel and IU-PDMS were self-healing. Benefited from the excellent performances of

as-prepared materials, the organohydrogel-based TENG could be endowed with environment resist and show better electrical output stability in a broad temperature range than the hydrogel-based TENG. Herein, the performances of the TENG device based on IU-PDMS with either organohydrogel (OG-TENG) or hydrogel (HG-TENG) were systematically investigated. Although the resistance of the organohydrogel electrode increased with temperature decreasing (the resistance in the range of 33 to 87 kΩ), there was little negative influence on the output performance of the OG-TENG, owing to its much larger inherent impedance (20 MΩ) [16]. The OG-TENG could be utilized to harvest mechanical energy at low temperature (Fig. 6a and 6d), showing a V_{oc} of 118 V and I_{sc} of 11 μA at -30 ^{o}C. As comparison, the HG-TENG has much poorer performance with the V_{oc} of 15 V and I_{sc} of 1.8 μA at -30 ^{o}C (Fig. 6b and 6e). The output performances of HG-TENG were largely degraded, which could be attributed to the frozen hydrogel. When the water in hydrogel is frozen, the conductivity of hydrogel would decrease severely [36]. The solid ice in the HG-TENG could easily slide the IU-PDMS film and seriously destroy the device after several mechanical impacts. The output performances of OG-TENG slightly dropped at low temperatures, due to the condensed water in air which could result in a leakage of charge. Overall, the OG-TENG still exhibited outstanding output performance at low temperatures, owing to the anti-freezing electrode and icephobic triboelectric layer. The organohydrogel would not be frozen, so the OG-TENG device at low temperature could be kept in the same state as at room temperature. Generally, when the TENGs are exposed in a cold environment, the formation of ice coating on the

triboelectric layer will impose a negative effect on the output performance of TENGs. The moisture in the ambient environment can be condensed into ice layer on the cold subject, which could lead to a decrease of the effective contact area. As the output performance of TENGs have strong relationship with the contact area between tribomaterials, the decrement of contact area will reduce the generation of triboelectricity. Fortunately, the IU-PDMS acting as tribomaterial was endowed with good icephobicity, which could prevent the ice accretion and maintain relatively high output performance.

After the OG-TENG and HG-TENG were stored at 80 ^{o}C for 10 hr, the output performances of the devices show remarkable opposite trend as shown in Fig. 6a to 6e. The OG-TENG has V_{oc} of 155 V and I_{sc} of 16 μA, while the HG-TENG cannot harvest energy at all. The main reason could be attributed to the loss of water in hydrogel at high temperature, which would depress the ion mobility in the polymer, and the dry gel lost its conductivity. Besides, after the water inside the HG-TENG was evaporated at high temperature, the film became fragile and was able to be easily broken as shown in Fig. 2f. However, the organohydrogel was heat-resistant, contributing to the stability of OG-TENG at high temperature. The temperature dependences of V_{oc} and I_{sc} from the two TENGs are presented in Fig. 6c and 6f, respectively. Comparing with the dramatic performance change of the HG-TENG along with temperature, the OG-TENG has much more stable performance in the measured temperature range, which can be utilized to harvest mechanical energy at

different temperature. As shown in Supplementary video I, the OG-TENG device could light 30 green LEDs up regardless of low or high temperature. Moreover, the OG-TENG showed outstanding repeatability and reliability during the heating-cooling cycle. In the third process of temperature changing from -30 ^{o}C to 80 ^{o}C (see Fig. S2 provided in Supplementary Information), the output performances almost maintained same as that in the first cycle. Contact electrification can be negatively affected at a very high temperature [37]. In the range of -30 ^{o}C to 80 ^{o}C, the thermal fluctuation has little effect on electron transport, resulting in the relatively stable electrical outputs.

As the organohydrogel and IU-PDMS had strong self-healing properties, the device structure could be easily recovered in the prepared TENG. The output performances of a self-healed OG-TENG at different temperature are shown in Fig. 6g and 6h. The relative devices were stored at different temperature, and then they were cut off from the middle, followed by bringing together to complete self-healing without any external stimuli. Compared with the results in Fig. 6a and 6d, the V_{oc} and I_{sc} almost recovers to their original level after the self-healing process. Here, the healing efficiency of the as-fabricated TENG is defined as the V_{oc} or I_{sc} of the healed sample to that of the original one. The healing efficiencies of the OG-TENG at different temperature are calculated and presented in Fig. 6i. The results reveal a very high healing efficiency above 95% at all the temperature regardless of V_{oc} or I_{sc}. Moreover, whether in high or low temperature conditions, the cracked OG-TENG device could

recover to its original electrical output performance within 1 s, which is the fastest compared with that of previously reported self-healing TENGs (the detail of comparison is presented in Table S1 of Supplementary Information). Due to the ultrafast recovery of the conductivity (Fig. 3f), the OG-TENG was endowed with remarkable self-healing performance in a wide temperature range. Generally, during the healing process, the output performance gradually recovers over time. While the ultrafast self-healing function could render the device performance without delay. In a word, the OG-TENG demonstrated an outstanding thermal stability and a strong self-healing ability thanks to the excellent properties of the organohydrogel and IU-PDMS.

3.7. Applications of Devices

It has been demonstrated that our fabricated OG-TENG has the characteristic of environment resist and ultrafast self-healing ability. Moreover, the materials utilized in OG-TENG comprise PAAM, nanoclay, glycerol, and PDMS, all of which have been proven to be nontoxic and used as biomedical materials [38-41]. Therefore, the environmentally friendly OG-TENG with multifunctional properties is highly suitable to be utilized as energy harvester for green mechanical energy and self-powered sensor to detect different human motion. The self-powered motion sensor based on OG-TENG in single-electrode mode was fabricated with 4 cm × 4 cm and installed underneath shoes to detect human walking at different temperatures. A container filled with dry ice and a heater was put on the ground to create the low temperature

and high temperature environment, respectively. For comparison, a same device was random cut by a surgical blade and stored at room temperature to perform self-healing reaction as the self-healed device. The performances of the original sensor and the self-healed sensor were measured at different temperature and motion styles, with their results presented in Fig. 7a and 7b, respectively. The V_{oc} can achieve at 26 V during walking and at 35 V during running. The varied values of V_{oc} at different human motion mode could be attributed to the change in contact area between tribomaterials. At running stage, feet may apply more force at device, leading to higher contact area which could increase the value of V_{oc}. Moreover, the motion frequency of running is faster than that of walking. The OG-TENG demonstrated stable and reliable performances under different circumstances, implying its good applicability as a motion sensor. The results show that the original and self-healed sensor can both be utilized to detect human motion. After transferring from AC into DC by using an inverter, a 4.7 μF capacitor could be utilized to store the generated electricity. The energy harvesting performance of the original and self-healed OG-TENG are shown in Fig. 7c and 7d. The two devices demonstrated similar behavior, which was that the charging speed at 25 ^{o}C and 80 ^{o}C was much faster than that at -30 ^{o}C. This could be attributed to the higher V_{oc} at high temperature. On the basis of the above results, the self-powered motion sensor based on OG-TENG is a promising sensor to detect different motion of human.

4. Conclusions

For practical applications, the durability and survivability of TENG in harsh working environments must be considered. Herein, we have developed a hydrophobic, icephobic, ultrafast self-healing TENG with thermal-resist, non-drying, non-freezing properties for energy harvesting and self-powered sensor. The prepared organohydrogel-based TENG presents electrical output stability in a wide temperature range, differing from previously reported hydrogel-based TENG which could be frozen at low temperature and dried in elevated temperature range, leading to capability loss of energy harvesting. The output performance of novel TENG could achieve at the open-circuit voltage, short-circuit current and short-circuit charge of about 157 V, 16 μA and 29 nC, respectively. The maximum value of output power density could achieve at 710 mW m^{-2}. Moreover, the broken device could rapidly recover to the initial electrical outputs within 1 s through self-healing process. This work will pave the way for novel applications of TENG in harsh environments with reliable output performance and self-healing durability for practical applications.

Acknowledgements

The research was financially supported by the National Natural Science Foundation of China through grants (51973119 and 21875190), the Natural Science Foundation of Guang Dong Province (2018A0303130060), the Science and Technology Innovation Commission of Shenzhen City (JCYJ20170818101245583), Shaanxi Natural Science Funds for Distinguished Young Scholars (2018JC-008), and PolyU PDFS (YW4N).

Appendix A. Supplementary data

Supplementary data to this article can be found online at xxx.

References

[1] J. Tollefson, Nature 508 (2014) 302-304.

[2] S. D. Collins, N. A. Ran, M. C. Heiber, N. Thuc-Quyen, Adv. Energy Mater. 7 (2017) 1602242.

[3] F. Di Giacomo, A. Fakharuddin, R. Jose, T.M. Brown, Energy Environ. Sci. 9 (2016) 3007-3035.

[4] X.-B. Cheng, R. Zhang, C.-Z. Zhao, Q. Zhang, Chem. Rev. 117 (2017) 10403-10473.

[5] Q. Zheng, B. J. Shi, Z. Li, Z. L. Wang, Adv. Sci. 4 (2017) 1700029.

[6] Z. L. Wang, Adv. Mater. 24 (2012) 280-285.

[7] C. Yan, Y. Gao, S. Zhao, S. Zhang, Y. Zhou, W. Deng, Z. Li, G. Jiang, L. Jin, G. Tian, T. Yang, X. Chu, D. Xiong, Z. Wang, Y. Li, W. Yang, J. Chen, Nano Energy 67 (2020) 104235.

[8] L.-B. Huang, W. Xu, J. Hao, Small 13 (2017) 1701820.

[9] W. Xu, L.-B. Huang, M.-C. Wong, L. Chen, G. Bai, J. Hao, Adv. Energy Mater. 7 (2017) 1601529.

[10] Y. Chen, X. Pu, M. Liu, S. Kuang, P. Zhan, Q. Hua, Z. Cong, W. Guo, W. Hu, Z. L. Wang, Acs Nano, 13 (2019) 8936-8945.

[11] L. Jin, X. Xiao, W. Deng, A. Nashalian, D. He, V. Raveendran, C. Yan, H. Su, X. Chu, T. Yang, W. Li, W. Yang, J. Chen, Nano Lett. 20 (2020) 6404-6411.

[12] C. Liu, Y. Wang, N. Zhang, X. Yang, Z. Wang, L. Zhao, W. Yang, L. Dong, L. Che, G. Wang, X. Zhou, Nano Energy 67 (2020) 104228.

[13] C. Liu, L. Fang, H. Zou, Y. Wang, J. Chi, L. Che, X. Zhou, Z. Wang, T. Wang, L. Dong, G. Wang, Z. L. Wang, Extreme Mech. Lett. 42 (2021) 101021.

[14] W. Xu, M.-C. Wong, J. Hao, Nano Energy 55 (2019) 203-215.

[15] L.-B. Huang, W. Xu, G. Bai, M.-C. Wong, Z. Yang, J. Hao, Nano Energy 30 (2016) 36-42.

[16] T. Liu, M. Liu, S. Dou, J. Sun, Z. Cong, C. Jiang, C. Du, X. Pu, W. Hu, Z. L. Wang, Acs Nano 12 (2018) 2818-2826.

[17] J. Sun, X. Pu, M. Liu, A. Yu, C. Du, J. Zhai, W. Hu, Z. L. Wang, Acs Nano 12 (2018) 6147-6155.

[18] L. Su, H. Y. Li, Y. Wang, S. Y. Kuang, Z. L. Wang, G. Zhu, Nano Energy 31 (2017) 264-269.

[19] J. Tian, H. Feng, L. Yan, M. Yu, H. Ouyang, H. Li, W. Jiang, Y. Jin, G. Zhu, Z. Li, Z. L. Wang, Nano Energy 36 (2017) 241-249.

[20] S. Chen, T. Huang, H. Zuo, S. Qian, Y. Guo, L. Sun, D. Lei, Q. Wu, B. Zhu, C. He, X. Mo, E. Jeffries, H. Yu, Z. You, Adv. Funct. Mater. 28 (2018) 1805108.

[21] P. Zhang, Y. Chen, Z.H. Guo, W. Guo, X. Pu, Z. L. Wang, Adv. Funct. Mater., 30 (2020) 1909252.

[22] L. Sun, S. Chen, Y. Guo, J. Song, L. Zhang, L. Xiao, Q. Guan, Z. You, Nano Energy, 63 (2019) 103847.

[23] Y. Lee, S.H. Cha, Y.-W. Kim, D. Choi, J.-Y. Sun, Nat Commun, 9 (2018) 1804.

[24] Q. Guan, G. Lin, Y. Gong, J. Wang, W. Tan, D. Bao, Y. Liu, Z. You, X. Sun, Z. Wen, Y. Pan, J. Mater. Chem. A 7 (2019) 13948-13955.

[25] X.P. Morelle, W.R. Illeperuma, K. Tian, R. Bai, Z. Suo, J. J. Vlassak, Adv. Mater. 30 (2018) 1801541.

[26] J. Yang, R. Bai, B. Chen, Z. Suo, Adv. Funct. Mater. 30 (2020) 1901693.

[27] X. Dai, Y. Du, J. Yang, D. Wang, J. Gu, Y. Li, S. Wang, B. B. Xu, J. Kong, Compos. Sci. and Technol. 174 (2019) 27-32.

[28] X. Dai, L.-B. Huang, Y. Du, J. Han, Q. Zheng, J. Kong, J. Hao, Adv. Funct. Mater., 30 (2020) 1910723.

[29] F. Chen, D. Zhou, J. Wang, T. Li, X. Zhou, T. Gan, S. Handschuh-Wang, X. Zhou, Angew. Chem. Int. Ed. 57 (2018) 6568-6571.

[30] Y. Liu, Y. Tian, J. Chen, H. Gu, J. Liu, R. Wang, B. Zhang, H. Zhang, Q. Zhang, Colloid. Surface. A 588 (2020) 124384.

[31] L.-B. Huang, G. Bai, M.-C. Wong, Z. Yang, W. Xu, J. Hao, Adv. Mater. 28 (2016) 2744-2751.

[32] X. Dai, Y. Du, Y. Wang, Y. Liu, N. Xu, Y. Li, D. Shan, B. B. Xu, J. Kong, ACS Appl. Polym. Mater. 2 (2020) 1065-1072.

[33] Y. Shen, X. Wu, J. Tao, C. Zhu, Y. Lai, Z. Chen, Prog. Mater. Sci. 103 (2019) 509-557.

[34] K. Golovin, S. P. Kobaku, D. H. Lee, E. T. DiLoreto, J. M. Mabry, A. Tuteja, Sci. Adv. 2 (2016) e1501496.

[35] J. Chen, J. Liu, M. He, K. Li, D. Cui, Q. Zhang, X. Zeng, Y. Zhang, J. Wang, Y. Song, Appl. Phys. Lett., 101 (2012) 111603.

[36] X. Li, H. Charaya, G. M. Bernard, J. A. W. Elliott, V. K. Michaelis, B. Lee, H.-J. Chung, Macromolecules 51 (2018) 2723-2731.

[37] X. Wen, Y. Su, Y. Yang, H. Zhang, Z. L. Wang, Nano Energy, 4 (2014) 150-156.

[38] Y. Ahn, H. Lee, D. Lee, Y. Lee, ACS Appl. Mater. Interfaces 6 (2014) 18401-18407.

[39] M. M. Reddy, S. Vivekanandhan, M. Misra, S. K. Bhatia, A. K. Mohanty, Prog. Polym. Sci. 38 (2013) 1653-1689.

[40] Y. Yang, L. Guan, X. Li, Z. Gao, X. Ren, G. Gao, ACS Appl. Mater. Interfaces 11 (2019) 3428-3437.

[41] R. Hinchet, S. W. Kim, ACS Nano 9 (2015) 7742-7745.

Figure captions:

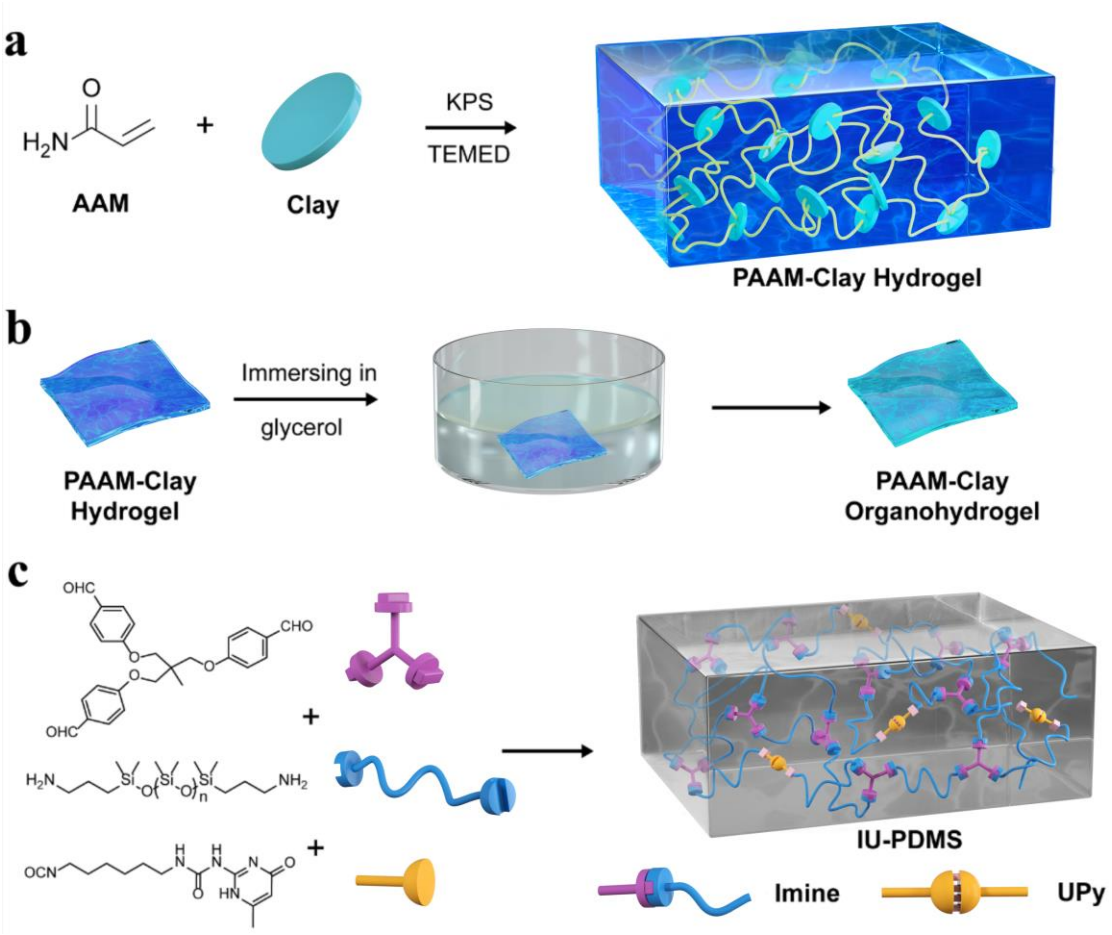

Fig. 1. Schematic illustration of the self-healing polymeric materials (PAAM-Clay organohydrogel and IU-PDMS). (a) Chemical structure of PAAM-Clay hydrogel through physical cross-linking (hydrogen bond). (b) Fabrication of PAAM-Clay organohydrogel from hydrogel by in-situ displacement with glycerol. (c) Synthetic route of IU-PDMS cross-linked by imine bond and UPy.

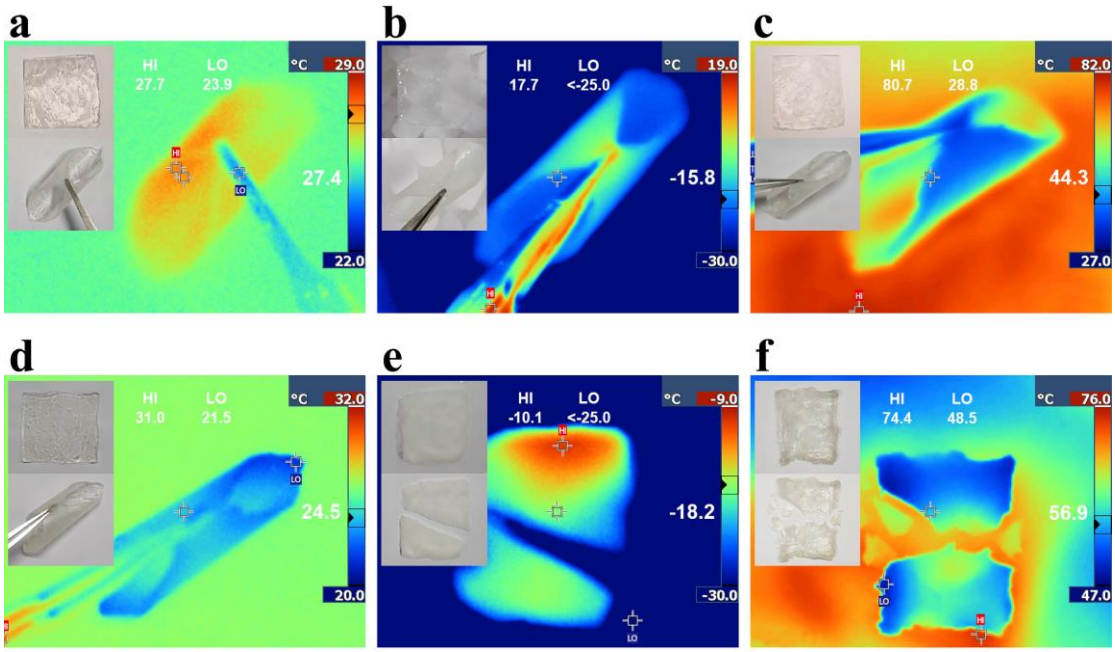

Fig. 2. Thermal images of glycerol-based PAAM-Clay organohydrogel at about (a) 25 ºC, (b) -30 ºC, and (c) 80 ºC. Thermal images of PAAM-Clay hydrogel at about (d) 25 ºC, (e) -30 ºC, and (f) 80 ºC. The insets are the optical images of each thermal image.

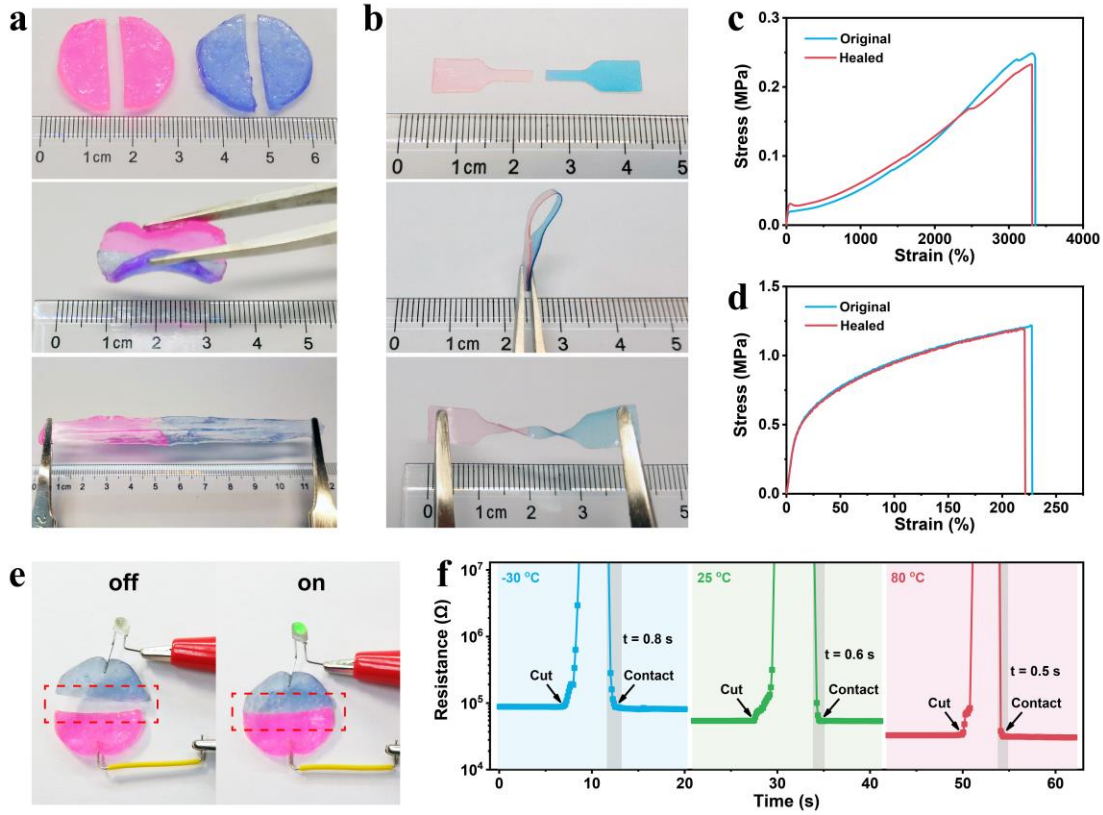

Fig. 3. Self-healing performances of PAAM-Clay organohydrogel and IU-PDMS. Optical images of the self-healing process for (a) glycerol-based PAAM-Clay organohydrogel and (b) IU-PDMS. Stress-strain curves of (c) glycerol-based PAAM-Clay organohydrogel and (d) IU-PDMS before and after self-healing. (e) Damaged and healed PAAM-Clay organohydrogel in series with an LED bulb under a voltage of 5 V. (f) Resistance variation during the process of cut and contact at different temperature (-30 ºC, 25 ºC, and 80 ºC).

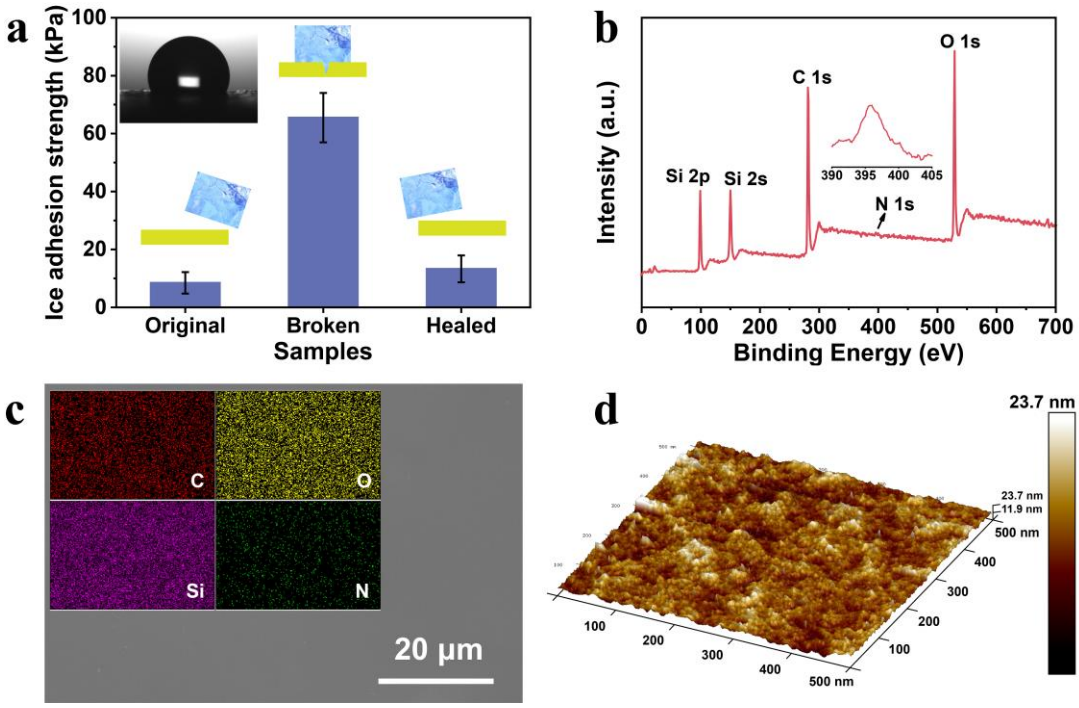

Fig. 4. Hydrophobic and icephobic behaviours of electrification layer of IU-PDMS. (a) Ice adhesion strength of the surfaces (the original, broken, and healed), with insets of the contact angle of the original sample, schematic illustration of the process of ice detachment, and mechanical interlocking between broken surface and ice. (b) XPS spectra, (c) SEM image with insets of elemental mapping images, and (d) AFM three-dimensional height images of IU-PDMS.

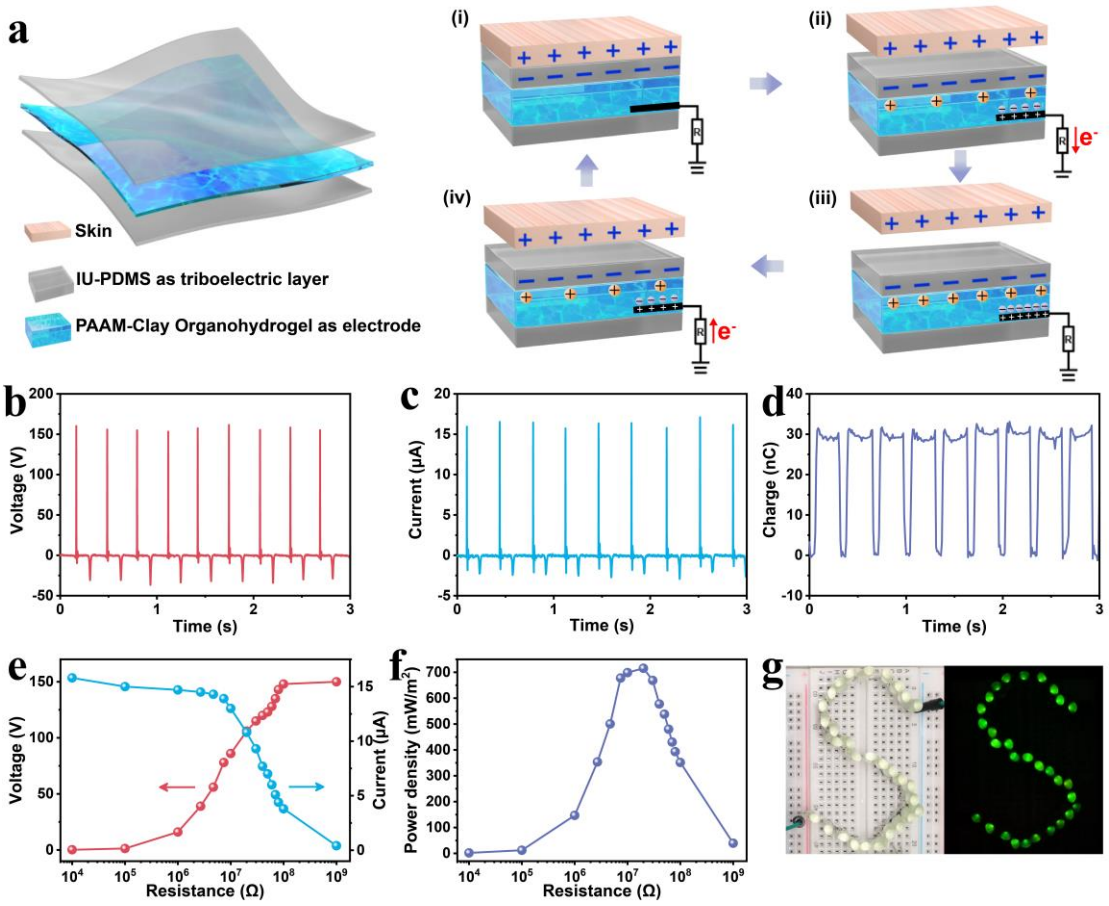

Fig. 5. Working mechanism and output performance of organohydrogel-based TENG. (a) Schematic of an organohydrogel-based TENG and the working principle of the device in single-electrode mode. (b) Open-circuit voltage, (c) Short-circuit current, and (d) short-circuit charge of the organohydrogel-TENG. (e) Output voltage and current versus resistance. (f) Variation of power density with external resistance. (g) Photograph of thirty green LEDs connected in series driven by the organohydrogel-TENG.

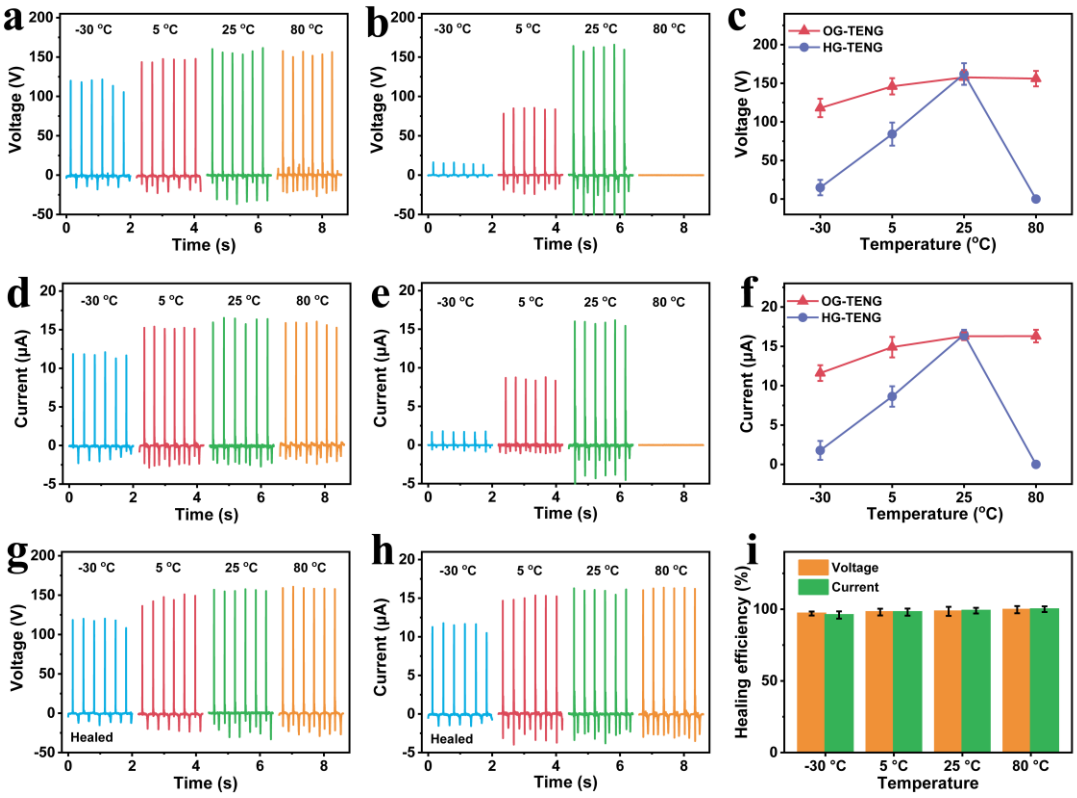

Fig. 6. Output performance of the organohydrogel-based and hydrogel-based TENGs under different temperature conditions. Open-circuit voltage of (a) OG-TENG and (b) HG-TENG at different temperature (-30 ^{o}C, 5 ^{o}C, 25 ^{o}C, and 80 ^{o}C). (c) Open-circuit voltage *vs* temperature of the OG-TENG and HG-TENG. Short-circuit current of (d) OG-TENG and (e) HG-TENG at different temperature (-30 ^{o}C, 5 ^{o}C, 25 ^{o}C, and 80 ^{o}C). (f) Short-circuit current *vs* temperature of the OG-TENG and HG-TENG. (g) Open-circuit voltage and (h) short-circuit current of self-healed OG-TENG at different temperature. (i) Healing efficiency of OG-TENG at different temperature.

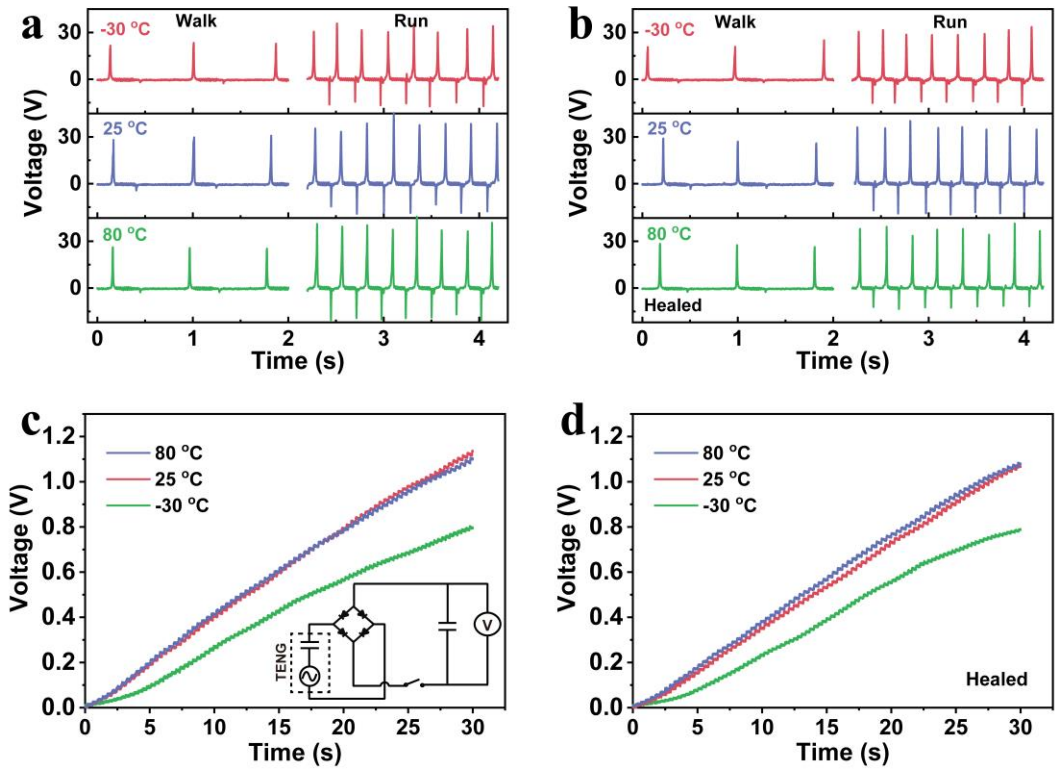

Fig. 7. Applications of the organohydrogel-TENG for self-powered sensor and biomechanical energy harvesting. Open-circuit voltage signals of the (a) original and (b) healed OG-TENG (attached on one foot) during walking and running under different temperature (-30 ºC, 25 ºC, and 80 ºC). Voltage profile of a 4.7 μF capacitor being charged by the (c) original and (d) healed OG-TENG under different temperature (-30 ºC, 5 ºC, 25 ºC, and 80 ºC). The inset in (c) is the equivalent circuit of the self-charging system.

Graphical abstract

An icephobic, and ultrafast self-healing TENG with thermal-resist, non-drying, and non-freezing properties is designed. The novel TENG shows excellent electrical output and stability at a wide temperature range from -30 ^{o}C to 80 ^{o}C. The ultrafast self-healing property of the device provides TENG with excellent recovery of electric output without delay. The proposed strategy is general, contributing to future sustainable energy and wearable devices.